

3-Arylisoxazolyl-5-Carboxylic Acid and 5-(Hydroxymethyl)-3-Aryl-2-Isioxazoline as Molecular Platforms for Liquid-Crystalline Materials

Aline Tavares,^a Paolo R. Livotto,^a Paulo F. B. Gonçalves^b and Aloir A. Merlo^{*a}

^aInstituto de Química, Universidade Federal do Rio Grande do Sul, 91501-970 Porto Alegre-RS, Brazil

^bCentro Universitário La Salle, 92010-000 Canoas-RS, Brazil

A síntese de uma plataforma molecular para materiais líquido-cristalinos derivados do ácido 3-arylisoaxazolil-5-carboxílico (**1**) e do 5-(hidroximetil)-3-aryl-2-isoxazolina (**2**) é descrita. Os intermediários **1** e **2** são obtidos através da reação de cicloadição [3+2] 1,3-dipolar entre arilóxidos de nitrilas e os dipolarófilos ácido acrílico e álcool alílico, respectivamente. Os compostos cristais líquidos são sintetizados através de uma estratégia de alongamento molecular do núcleo primitivo isoxazolinico pela conexão de subunidades arilacetilênicas, as quais foram obtidas da reação de Sonogashira. Sob essas condições, séries de cristais líquidos **5a-c**, **6**, **7a-g** e **8a-d** têm sido sintetizadas com rendimentos de médios para bons. Os compostos finais apresentam propriedades líquido-cristalinas nematogênica e esmectogênica. Um cálculo DFT no nível B3LYP/6-31G(d,p) é também apresentado e alguns parâmetros estruturais obtidos são analisados.

The synthesis of the molecular platform for liquid-crystalline materials based on 3-arylisoxazolyl-5-carboxylic acid (**1**) and 5-(hydroxymethyl)-3-aryl-2-isoxazoline (**2**) is described. The key intermediates **1** and **2** are obtained by [3+2] 1,3-dipolar cycloaddition reaction between an aryl nitrile oxide and an acrylic acid and allylic alcohol as the dipolarophile. The liquid crystals (LC) compounds are synthesized through a “molecular elongation strategy” from the initial isoxazolinic core by connecting the arylacetylene moiety obtained from the Sonogashira reaction. Under these conditions, the series of liquid crystals **5a-c**, **6**, **7a-g** and **8a-d** have been successfully synthesized in fair to good yields. The final compounds display nematic and smectic liquid-crystalline properties. The structural properties of the series of the liquid crystals has been studied using DFT methods at level B3LYP/6-31G(d,p). The equilibrium geometries in the gas phase are presented and analyzed.

Keywords: 3,5-disubstituted isoxazolines, [3+2] 1,3-dipolar cycloaddition, liquid crystals, molecular platform

Introduction

The [3+2] 1,3-dipolar cycloaddition reaction of a nitrile oxide to an alkene or alkyne has proven to be extremely useful in the preparation of a variety of compounds in organic chemistry. Among the various classes of compounds which are prepared from these cycloadducts are enones,¹ 1,3-amino alcohols,² β,γ -dihydroxy ketones³ and β -hydroxy ketones.⁴ In the area of materials, the construction of the isoxazoline and isoxazole rings by this methodology constitute an easy way to prepare a molecular platform for the synthesis of smart molecules, such as polymers and non-polymer liquid-crystalline materials.⁵

Our previous results showed that the introduction of an isoxazoline ring flanked by aromatic rings or polar groups opened a route to prepare useful intermediates in the field of liquid crystals.⁶ Herein we describe the preparation of four homologous series of 3,5-disubstituted isoxazoline rings. A complete study of the thermal behavior of these compounds is also presented with the goal to understanding the correlation between the molecular structure and liquid crystal parameters.

Based upon the considerations discussed above, we now report a convenient and practical route to the synthesis of isoxazoline ring platform for liquid crystal (LC) materials. The compounds from series **5** and **6** are derived from 3-arylisoxazolyl-5-carboxylic acid (**1**) while the members of the homologous series **7** and **8** are derived from 5-(hydroxymethyl)-3-aryl-2-isoxazoline (**2**).

*e-mail: aloir@iq.ufrgs.br

Results and Discussion

Synthesis

To synthesize the isoxazoline LC, the molecular platforms **1** and **2** bearing carboxyl or hydroxyl groups suitable for further derivation were prepared (Chart I). The acid **1a-d** and alcohol **2a-d** were obtained using [3+2] 1,3-dipolar cycloadditions according to reference 6.

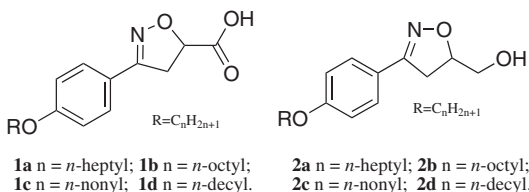
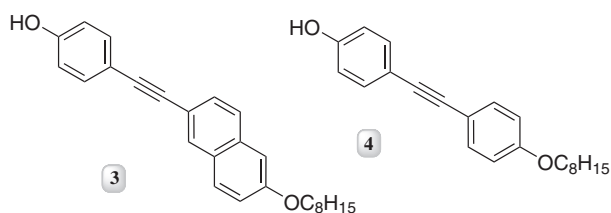
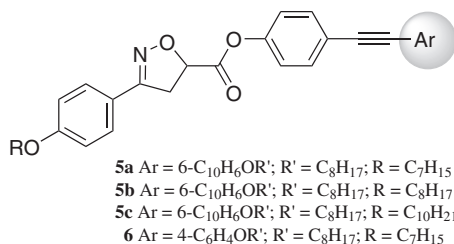


Chart I. The isoxazoline platforms **1** and **2**.

To achieve our goal of the isoxazoline LC material it was necessary to synthesize the phenols **3** and **4** as the chemical counterparts of the acid **1**. The synthesis of the key intermediates **3** is reported elsewhere.⁶ Compound **4** was prepared following the experimental procedure to **3**.

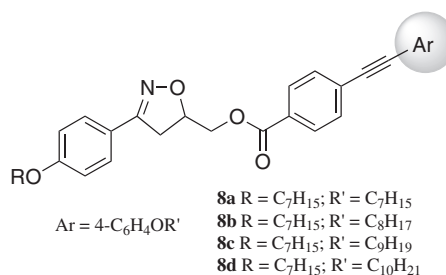
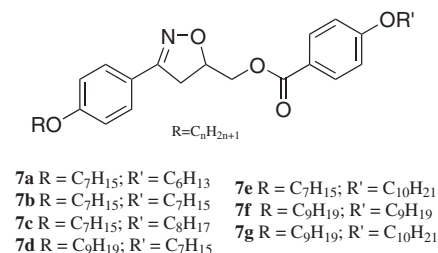


The chemical connection between the intermediates **3** and **4** and acid **1** was made through an esterification reaction using the DCC-DMAP protocol. Thus, the compounds **5a-c** and **6** were synthesized as representative members of these homologous series.



The third and fourth homologous series **7a-g** and **8a-d** are derived from 5-(hydroxymethyl)-3-aryl-2-isoxazoline (**2**). The compounds **7a-g** were quickly prepared by an esterification reaction (DCC/DMAP) between the corresponding *p*-*n*-alkoxybenzoic acid⁷ and the alcohol **2**. In order to synthesize the elongated (anisotropic) liquid-

crystalline isoxazolines **8a-d**, we again applied the DCC/DMAP protocol to introduce the ester linkage by reaction of *p*-bromobenzoic acid with the alcohol **2a**. To accomplish the synthesis of the homologous series **8a-d** the triple bond was inserted through the Sonogashira cross-coupling reaction between the 1-alkoxy-4-ethynylbenzene⁸ and the ester derived from *p*-bromobenzoic acid.



Liquid-crystalline behavior

Thermal analysis of all isoxazolines **5a-c**, **6**, **7a-g** and **8a-d** was performed by differential scanning calorimetry (DSC). The texture of the mesophase⁹ was identified by microscopy studies on cooling from the isotropic liquid state of the samples (Figure 1). The transition temperatures and enthalpy values were collected from a second heating scan and is compiled in Table 1. Polarizing optical photomicrographs of the representative LCs are shown in Figure 1. The 3-phenylisoxazolyl-5-carboxylate esters **5a-c** exhibited enantiotropic liquid-crystalline properties (Figures 1a and 1b). The ester **6** did not exhibit mesomorphic behavior under optical polarized light microscopy (Figure 1c). The LC 5-(hydroxymethyl)-3-aryl-2-isoxazolyl benzoates **7c-g** and **8a-d** displayed monotropic liquid-crystalline phase where the smectic C and nematic mesophases were observed in these series (Table 1), respectively.

The mesophase characterization was made by polarized optical microscopy studies (POM, Figure 1) and the enthalpy values were obtained from DSC traces (Figure 2). The schlieren textures of series **5a-c** and **7d-g** show singularity lines with two and four dark brushes, which correspond to the extinction orientation of the

Table 1. Transition temperatures (°C) for homologous series **5a-c**, **6**, **7a-g** and **8a-d** and enthalpies values (ΔH , kcal mol⁻¹)

Entry	R/R' C _n H _{2n+1}	Phase Transition Temperatures / (°C)		ΔT^d	Enthalpies values		
		Heating	Cooling		Melt ^e	Iso-phase-K ^d	
5a	7/8	K 144.5 ^a N 148.0 ^a I	I 142.9 N 136.9 K	3.5	6.74	I 0.015 N 6.59 K	
5b	8/8	K 134.4 ^a N 150.5 ^a I	I 144.0 N 127.3 K	16.1	6.05	I 0.031 N 6.00 K	
5c	10/8	K 142.6 ^a N 151.0 ^a I	I 149.5 ^a N 130.7 K	8.4	5.93	I ^f N 6.01 K	
6	7/8	K 129.5 I	I 116.1 K	-	12.31	I 12.74 K	
7a	7/6	K 100.8 I	I 73.7 K	-	13.07	I 12.87 K	
7b	7/7	K 97.8 I	I 73.7 K	-	15.10	I 15.29 K	
7c	7/8	K 96.7 I	I 78.6 ^{b,c} K	-	12.64	I 12.64 K	
7d	9/7	K 93.8 I	I 76.9 ^b SmC 64.8 K	12.1	18.69	I 4.19 SmC 10.88 K	
7e	7/10	K 102.5 I	I 75.7 ^b SmC 71.2 K	4.5	13.40	I 2.81 SmC 11.79 K	
7f	9/9	K 91.9 I	I 82.5 ^b SmC 58.1 K	24.4	12.79	I 3.01 SmC 6.15 K	
7g	9/10	K 100.4 I	I 83.3 ^b SmC 68.2 K	15.1	16.67	I 3.66 SmC 11.82 K	
8a	7/7	K 134.7 I	I 125.8 ^{a,b} N 118.0 K	7.8	6.26	I ^f N 8.36 K	
8b	7/8	K 138.4 I	I 134.3 ^b N 120.2 K	14.1	13.91	I 0.67 N 13.53 K	
8c	7/9	K 133.5 I	I 120.0 ^b N 116.7 K	3.3	15.01	I 0.087 N 15.66 K	
8d	7/10	K 137.8 I	I 132.5 ^b N 121.4 K	11.1	11.94	I 0.72 N 11.01 K	

Scan rate: 10 °C min⁻¹ for all samples; K = Crystal phase; SmC = Smectic C phase and N = Nematic phase. ^aTransition temperatures were obtained from POM analyze. ^bMonotropic behavior. ^cEnthalpies values (second heating/cooling stage) were determined from crystal phase to LC phase or isotropic phase for compound **6**. ^dHeating for **5a-c** and cooling for **7a-g** and **8a-d**. ^eUpon slow cooling the samples crystallizes. Upon fast cooling the sample displayed a very short range of the SmC phase during the crystallization process. ^fEnthalpy value not determined.

liquid crystals. The singularity points are defects in the structure where two or four brushes meet. In the smectic C phase, only singularities with four brushes are observed (Figures 1e and 1f). Nematic phase may also showed singularities with two brushes (Figures 1a and 1b).

The homologous series **8a-d** exhibited a thread-like texture when the sample was sandwiched between two glass plates that had not been rubbed or treated (Figure 1d). This texture is usually observed in thin samples placed between two crossed polarizers. The dark lines, the so-called threads, are line singularities, which either connect two point defects or form closed loops. The planar thread-like texture is characteristic of liquid-crystalline nematic phase.

Compounds **5a-c** displayed enantiotropic nematic phase whereas compound **6** is a non-mesomorphic compound. The non-liquid crystal **6** melts at 129.5 °C from its crystalline state to an isotropic liquid and it crystallizes at 116.1 °C without any trace of a LC mesophase (Figures 1c and 2). The lack of LC behavior for this compound is probably related to the geometrical anisotropy when the naphthyl group is changed to phenyl group.

Compounds belong to **5a-c** series showed enantiotropic behavior when analyzed by POM. However, the DSC traces of the **5a** did not exhibit K → N on heating and whereas **5c** did not exhibit I → N on cooling (Figure 2). For example, on heating, the sample **5a** enters into the nematic phase

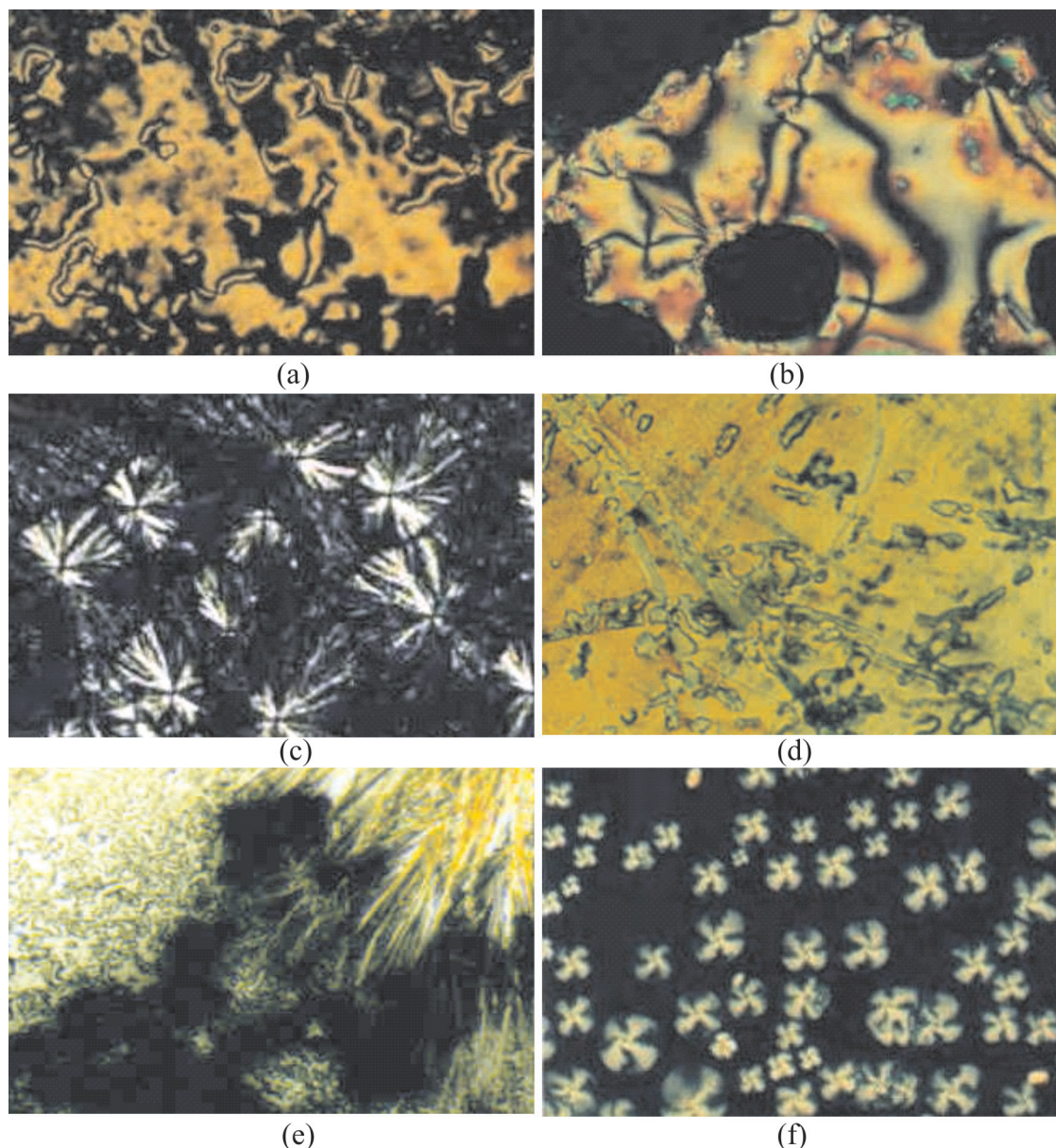


Figure 1. Polarizing optical photomicrographs (10x). (a) The planar thread-like texture on cooling of **5a** (141.7 °C); (b) schlieren texture of **5b** on heating (145.8 °C); (c) crystal phase (“pom-pom” texture) of **6** on cooling (107.8 °C); (d) nematic planar texture of **8d** on cooling (129.7 °C); (e) the coexisting of smectic C and crystal phase of **7d** on cooling (67.2 °C); (f) the schlieren texture of the smectic C phase (color-four-fold rosette and black-isotropic liquid) of **7g** on cooling (83.0 °C).

at 144.5 °C and melts to an isotropic liquid at 148.0 °C. The range of temperature for the mesophase is small for **5a** ($\Delta T = 3.5$ °C) and large for **5b** ($\Delta T = 16.1$ °C) and **5c** ($\Delta T = 8.4$ °C). On cooling, the mesophase range follows the same tendency. They are larger for compounds **5b** ($\Delta T = 16.7$ °C) and **5c** ($\Delta T = 18.8$ °C) than for **5a** ($\Delta T = 6.0$ °C), while the transition enthalpies (Table 1) for the isotropic to nematic transition of the **5a-c** are rather low. These values are consistent with a less ordered nematic mesophase.

The third homologous series **7a-g** displayed a monotropic smectic C mesophase only for the superior

members **7c-g**. For the first and second members (**7a** and **7b**) of this series no mesophase was observed. While the next member **7c** exhibited a monotropic smectic C phase. The smectic C phase appeared only under fast cooling and the mesophase range was too short to be determined under these conditions. On cooling, **7c** crystallizes at 78.6 °C. The broken-fan focal conic texture of the SmC phase appears during the crystallization process. The broken-fan can be visualized simultaneously with the crystals and they disappear very fast. This situation makes it impossible to get some information about the range of this mesophase. Upon slow cooling, no traces of the mesophase were detected and

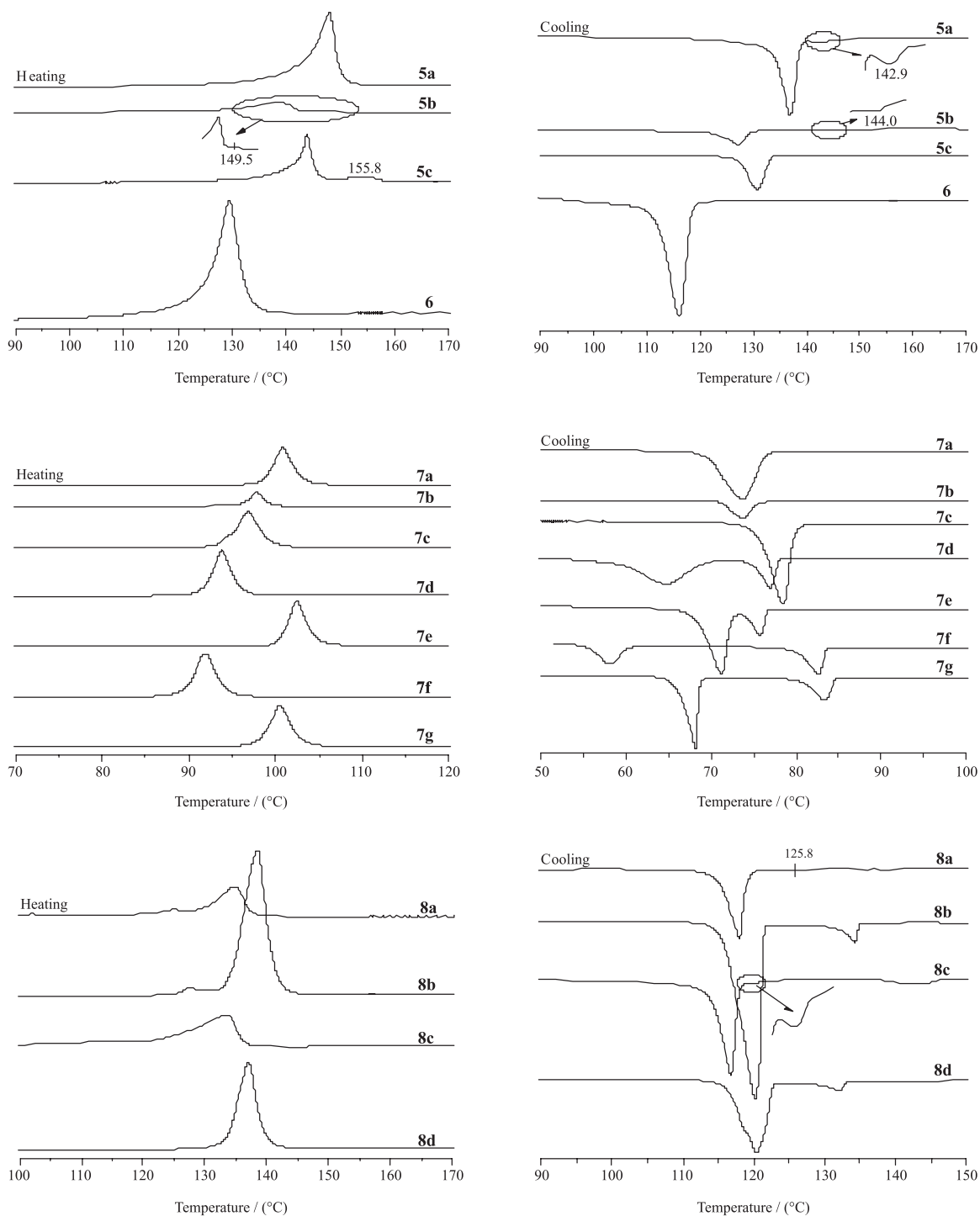


Figure 2. DSC thermograms of compounds **5a-c**, **6**, **7a-g** and **8a-d** on 2nd cycle at 10 °C min⁻¹.

observed. For the superior members **7d-g** the range of the monotropic SmC phase was determined. The DSC traces are shown in Figure 2 and the thermal data for this series is shown in Table 1. The melting points of these compounds display a regular tendency if we compare them in *pairs*. The compounds containing odd carbon atoms in their alkyl chains melt at higher temperatures than the next member

having an even carbon in the alkyl chains. For instance, the melting points of **7a**, **7c**, **7e** and **7g** are higher than **7b**, **7d** and **7f**. Figure 3a shows the dependence of the melting points on the number of carbon atoms in the alkyl tail for the **7a-g** homologues. Also, from Figure 3a it is possible to see that the melting point decreases with the increase of *n* in the alkyl chain on going from **7a** to **7d**. The melting point

for **7e** doesn't follow the tendency, and it is higher than **7d**. However it is possible to establish the same correlation between the melting point and the length of the terminal *n*-alkyl chain to the last three members of this series. For instance **7e** with an odd number of carbon atoms in its alkyl chain has a higher melting point than **7f**. The melting points of compounds **7e-g** display an odd-even effect as seen with the four first compounds. The deviation observed jumping from **7a-d** to **7e-g** may be associated with the increase in the molecular weight of the latter compounds. The tendency observed in both groups of the LC series **7a-d** and **7e-g** related to the lowering of the melting point is probably a manifestation of the lipophilic effect as the length of the alkyl chains increase. The transition enthalpies of the isotropic to smectic transitions of **7d-g** are higher than for both **5a-c** and **8a-d**. The enthalpy value suggests a more ordered phase going from isotropic to smectic phase compared to compounds **5a-c** or **8a-d**.

In general, as the length of the alkyl chains increases the mesophase range becomes wider, especially with respect to smectic phase; the opposite is observed for the nematic phase (see discussion for **8a-d** below). The reduction of the length of the alkyl chain may be responsible for the absence of the mesophase. A delicate balance between many structural parameters favors the appearance of the mesophase for the intermediate compounds **7c-g**. The inversion of the ester group and the insertion of a methylene unit between the isoxazolyl and carboxyl groups are other two factors that should have considered when we compare the compounds **7a-g** with **5a-c** and **6**.

In contrast to the compounds **5a-c**, the homologous series **8a-d** displayed monotropic nematic mesophase with planar thread-like texture. The thermal, optical and thermodynamic data of these compounds are compiled in Table 1. All compounds displayed similar thermal behavior. The DSC traces are shown in Figure 2. For **8a** and **8c** ($\Delta T = 7.8$ °C; $\Delta T = 3.3$ °C) the mesophase range was smaller than for **8b** and **8d** ($\Delta T = 14.1$ °C; $\Delta T = 11.1$ °C). The melting points of this series have the same tendency observed to the series **7a-g**. The LCs **8a** and **8c** melt at lower temperature than **8b** and **8d**. The LCs with odd carbon atoms in the alkyl group, considering R plus R', melt *ca.* 4 °C above the LCs containing even carbon atoms on their terminal tails. The transition temperatures I \rightarrow N obtained on cooling exhibited the same behavior. For example, on cooling, **8b** and **8d** enter into the nematic phase at higher temperature than **8a** and **8c**.

The usual even-odd alternations of temperature range of the crystal-isotropic phase and of the isotropic-nematic phase transition are observed. For the odd number of the carbon atoms the mesophase range is higher than for the

even number of the carbon atoms in the alkyl tail. Figure 3b shows the dependence of the transition temperatures on the number of carbon atoms in the alkyl tail for the **8a-d** series. The tendency observed upon heating of the melting points is similar to the transition temperatures I \rightarrow N observed on cooling process. The compounds that have an odd number of carbon atoms exhibit higher values than for those with an even number of carbon atoms. This can be seen in Figure 3b: the superior line is related to the melting point and inferior line is associated with the temperature when the compounds **8a-d** enter into nematic phase. It should be noted that, when compared with **8b** and **8d**, the enthalpy values for these isotropic-nematic transitions of **8c** also showed the odd-even effect. The enthalpy value of the **8a** was too small to be detected by DSC. The phase transition for this member was observed with a polarizing microscope. However the values for the compounds with odd carbon atoms in the alkyl tail, **8b** and **8d**, are larger than the conventional nematic \leftrightarrow isotropic transition enthalpies (< 0.50 kcal mol⁻¹) for calamitic liquid crystals. In addition, these enthalpy values for compounds **8a-d** are higher than series **5a-c**. This may be indicating that relatively strong intermolecular interactions might exist in its nematic phase and could be attributed to the inversion of the carboxylate group between **5a-c** and **8a-d**.

A theoretical study was performed in order to understand the phase behavior and correlate it to the structural features of these compounds. We selected the LC compounds **5b**, **7b** and **8c** as a representative of this study and their energy and its corresponding geometry of all model systems were obtained by full optimization without any constraint. The calculation was performed with the GAUSSIAN 98¹⁰ program using the B3LYP hybrid functional,¹⁰ employing a 6-31G(d,p) basis set.

The molecular shape of a compound has a critical effect on its liquid-crystalline behavior. Two facts are important and need to discuss relating to the mesomorphic behavior of the calamitic liquid crystals (rod-like mesogen). First, the linear-shape of the calamitic LC changes to a bent-shape with the introduction of five-membered heterocycles into the center of the mesogenic core.¹¹ The bent-shape is a consequence of the relative position of the substituent bonded at the heterocyclic group. So, the deviation of linearity is an important structural parameter that should be taken into account. Second, the 3,5-disubstituted isoxazoline ring has two non-coplanar aromatic groups bonded at 3- and 5-position of the isoxazoline ring. The non-linearity of the isoxazoline ring along with the non-coplanarity of the two aryl groups located at C₃ and C₅ on the heterocyclic ring are determine whether a stable liquid-crystalline phase forms. To minimize this unfavorable disposition of the groups in

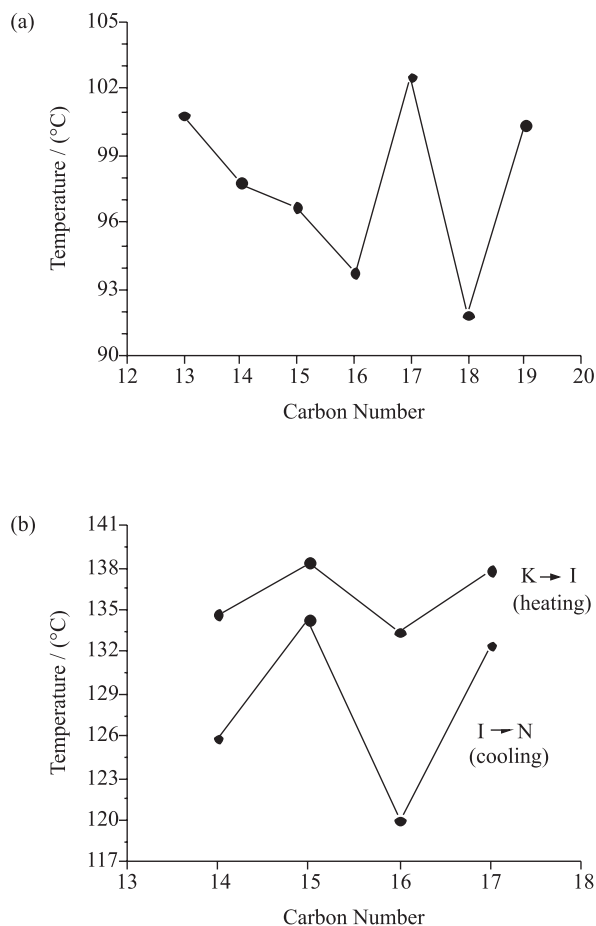


Figure 3. (a) Plot of melting point against the number of carbon atoms of the homologues **7a-g**. (b) Plot of transition temperatures against the number of carbon atoms (n) in the alkoxy chain of the compounds **8a-d**. Melting points (above); I-N transition temperature (below, on cooling).

the 3- and 5-carbon atom of the isoxazoline ring, the final central core must be as long as possible and possess high polarizability. In this way, the potential LC materials are reached through an “elongating molecular strategy” from the isoxazoline intermediates. This elongation builds off the rigid isoxazoline core to form a more polarizable and mesogenic one.

The mesomorphic behavior found in this work is due to the presence of the long aromatic moiety laterally bonded to the isoxazoline ring. However, in some cases the molecular dimensions (length-to-breadth ratio) of the aromatic moiety are not sufficient to overcome the non-coplanarity of the aryl group connected on the isoxazoline ring. In this situation no mesophase or unstable mesophase (*i.e.*, monotropic behavior) appears. By changing the hybridization of the C_4 and C_5 carbon atoms of the isoxazolinic system the liquid-crystalline state forms vigorously. Our previous work showed that oxidation of the isoxazoline to isoxazol ring yield LC materials with a large enantiotropic nematic mesophase.⁶ The appearance of stable mesophase in

isoxazol systems¹² is due to the substitution of a tetrahedral to planar carbon in the heterocyclic so that the two aryl and the isoxazolyl groups are coplanar and thus fully conjugated.

Table 2 shows the three lowest-energy conformations of the **5b**, **7b** and **8c** compounds. The other conformations of these compounds are not energetically favorable (by more than 1.00 kcal mol⁻¹) and these contributions can be neglected because they are local minima. The energy profile of the conformational population largely favors the conformation shown in Table 2. Therefore, we focused our analysis on the lowest-energy conformations so that the high energy conformations are not considered during this study. Modeling of these structures allows certain interesting conclusions to be drawn concerning their mesomorphic behavior. The distance between the oxygen of the carboxylate group and the hydrogen ($O_{45}-H_{42}$) for the **5b**, $O_{44}-H_{39}$ for the **7b** and **8c** are 2.37, 2.46 and 2.45 Å, respectively. These values reveal a weak hydrogen bond in these conformers and they supported that this interaction is important to maintain the conformers in their lowest-energy state. As we can see in the Figure 4a, the hydrogen atom bonded to carbon 4 in the isoxazolinic ring shows a more positive charge than the others, interacting to the carboxylic oxygen as a weak hydrogen bond.

The dipole moment of these conformers may also play an additional role in the stabilization of the mesomorphic state. Compound **5b** has the lowest value whereas **8c** presents the highest value. A probable conclusion about this data is that compounds having the smallest molecular dipole values display enantiotropic behavior as we can see from the data for series **5a-c** (Table 1). On the other hand, compounds belonging to the series **7a-g** and **8a-d** having high values of the molecular dipole show monotropic LCs. A preliminary conclusion from the modeling data is that a large increase in the molecular dipole does not favor the formation of an enantiotropic mesophase (Table 1). However it is important to point out that monotropic behavior, or the absence of a mesogenic state, observed in the series **7a-g** and **8a-d** is mainly due to the deviations of the coplanarity between aromatic molecular segments connected by the polar isoxazoline ring.

The dihedral angle of the **5b**, **7b** and **8c** conformers was selected and they are listed in Table 2. The theoretical calculations reveal that rotation about C_1-C_{44} and C_1-C_{41} bond of the compounds **5b**, **7b** and **8c**, respectively, play an important role on their corresponding liquid crystalline behavior. The rotation about the C_1-C_{44} bond of **5b** yielded the more stable conformer which is separated by more than 1.00 kcal mol⁻¹ from the another unstable conformer of **5b** (not shown). The angle between two planes (right and left) of the molecule is about 135.9°. The dihedral angle

$O_2-C_1-C_{44}-O_{45}$ to the most stable conformation is 116.1° . This molecular arrangement favors mesophase formation probably due to the tendency of the polar mesogenic phase to self-assemble during the melting or passing from the isotropic to mesogenic state.

The insertion of methylene unit between the isoxazoline ring and carboxyl group changes the relative disposition of the two planes in the conformers of **7b** and **8c**. As we can see in Table 2 the conformers **7b** and **8c** present two distinct planes connected by the C_1-C_{41} bond. These planes are slightly collinear, twisted and non-coplanar. The estimated angles between these planes are 30.47° for **7b** and 28.45° for **8c** (Figure 4b,c). The dihedral angles $O_2-C_1-C_{41}-O_{42}$ to the most stable conformation of the **7b** and **8c** are 163.5° and 163.3° , respectively. This arrangement favors the short-weak hydrogen bond interaction between $O_{44}-H_{39}$ atoms in both rotamers. The conclusion that can be drawn from these data is that the methylene unit, as described above,

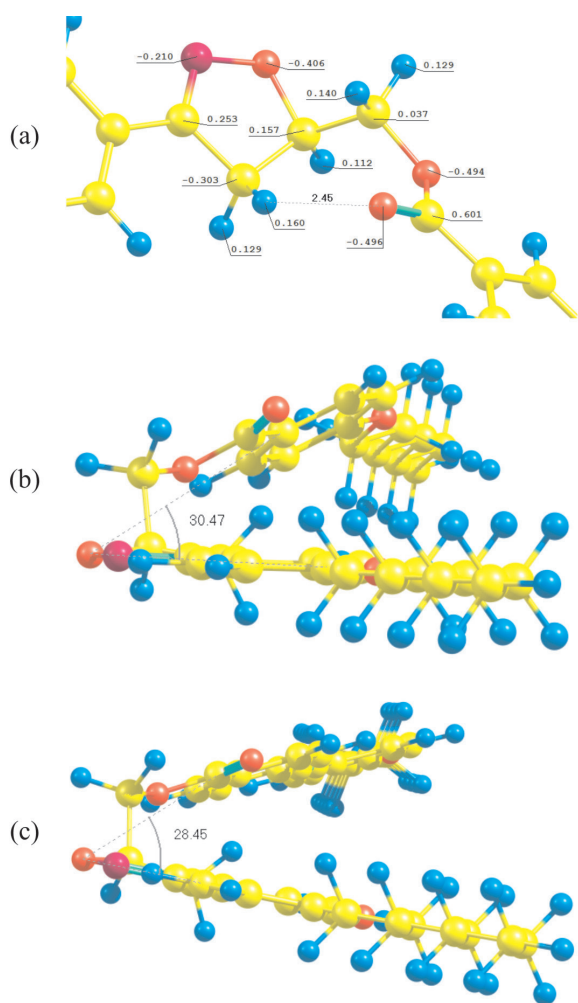


Figure 4. (a) Central core of the **8c** molecule showing the Mulliken charges and distance between oxygen of the carboxylate group and the hydrogen (2.45 Å, dotted line). (b) and (c) Dihedral angle between molecular planes of the conformers: 30.47° for **7b** and 28.45° for **8c**.

produces two distinct planes which disfavor the molecular interaction in the liquid-crystalline state. The electrostatic interaction and dispersion interaction (van der Waals forces, π -stacking effects, etc) cannot compensate for the structural constraints that are imposed by the methylene group in the 5-(hydroxymethyl)-3-aryl-2-isoxazoline ring.

Experimental

Materials

Ethanol, diethyl ether, *p*-bromobenzoic acid, copper(I) iodide (CuI), triphenylphosphine (PPh_3), 4-(*N,N*-dimethylamino)pyridine (DMAP) and 1,3-dicyclohexylcarbodiimide (DCC) were used without further purification from Aldrich. The *p-n*-alkoxybenzoic acid and 1-alkoxy-4-ethynylbenzene were prepared according to references 7 and 8, respectively. *Bis*-(triphenylphosphine)palladium (II) chloride [$PdCl_2(PPh_3)_2$] was prepared following the procedure reported in reference 13. Triethylamine (Et_3N) was distilled over potassium hydroxide. Tetrahydrofuran (THF) was dried over sodium metal-benzophenone and distilled immediately before use. Anhydrous sodium sulphate (Na_2SO_4) was used to dry organic extracts.

Characterization

Nuclear magnetic resonance spectra were obtained on a Varian 300 MHz instrument. Chemical shift are given in parts *per million* (δ) and are referenced from tetramethylsilane (TMS). GC-MS spectra are obtained using a Varian Saturn 2100T CG-MS equipped with a 100 meter CP Sil Pona CB (0.25 mm) column. The column temperature is started at $50^\circ C$ and is gradually ramped to $230^\circ C$ ($15^\circ C\ min^{-1}$) until the end of the run. Infrared spectra were recorded on a Perkin-Elmer Spectrum One FTIR Spectrometer Instruments using NaCl plates in case of solids (nujol dispersions) and as thin film supported between NaCl plates in case of liquids and are reported as wavenumber (cm^{-1}). Elemental analyses were performed on a Perkin-Elmer model 2400 instrument. All new compounds **5a-c**, **6**, **7a-g** and **8a-d** gave satisfactory spectral, MS data and elemental analysis. The DSC analyses were obtained on a DSC 2910 TA Instruments.

Thermal characterization

Melting points, thermal transitions and mesomorphic textures were taken using an Olympus BX41 microscope equipped with a Mettler Toledo FP82 Hot Stage FP90

304, 290, 279, 258, 233, 218 (100), 190, 129, 128, 116 and 91.

4-[(4-Octyloxyphenyl)ethynyl]phenyl 3-(4-heptyloxyphenyl)-4,5-dihydroisoxazole-5-carboxylate (6)

This compound was obtained by procedures similar to those used to prepare compound **5a**. Yield: 110 mg, 50%; white solid; mp 129.5 °C; Anal. Found: C, 76.58; H 7.68, N 2.42; calc. for C₃₉H₄₇NO₅: C, 76.82; H, 7.77; N, 2.30%; IR ν_{\max} /cm⁻¹: 2924, 2855, 1765, 1595, 1467, 1378, 1224, 1043, 896, 859, 820, 722, 666; ¹H NMR (300 MHz, CDCl₃) δ 0.88 (m, 6H, (CH₃)₂), 1.40 (m, 18H, (CH₂)₉), 1.78 (m, 4H, (CH₂CH₂O)₂), 3.75 (m, 2H, CH₂CH), 3.98 (m, 4H, CH₂O), 5.37 (dd, 1H, CH₂CH, *J* 7.2, 10.5 Hz), 6.86 (d, 2H, Ar, *J* 8.4 Hz), 6.93 (d, 2H, Ar, *J* 8.4 Hz), 7.13 (d, 2H, Ar, *J* 8.4 Hz), 7.44 (d, 2H, Ar, *J* 8.4 Hz), 7.52 (d, 2H, Ar, *J* 8.4 Hz), 7.64 (d, 2H, Ar, *J* 8.4 Hz); ¹³C NMR (75 MHz, CDCl₃) δ 14.0, 14.1, 22.6, 22.7, 25.9, 26.0, 29.0, 29.1, 29.2, 29.3, 29.4, 31.7, 31.8, 39.3, 68.1, 68.2, 77.8, 87.0, 90.0, 114.5, 114.8, 120.5, 121.3, 121.9, 128.6, 132.6, 133.0, 149.8, 155.7, 159.3, 161.1, 168.6; EI-MS: *m/z* 609 [M⁺], 496, 494, 480, 418, 380, 349, 321, 306, 305, 288, 258, 233, 218 (100), 205, 191, 129, 115 and 91.

General procedure for synthesis of homologue series 7a-g

The corresponding alcohol **2a** or **2c** (5.8×10^{-4} mol) and the respective *p-n*-alkoxybenzoic acid (5.8×10^{-4} mol) were suspended in dry THF (5 mL) and stirring for 15 min under argon atmosphere. Then DCC (8.7×10^{-4} mol) and DMAP (7.6×10^{-5} mol) were added. The reaction mixture was stirred for 24 h at room temperature. The white precipitate was filtered off and washed with THF. The solvent was removed and the crude product was recrystallized from ethanol (double recrystallization).

Representative data for [3-(4-heptyloxyphenyl)-4,5-dihydroisoxazol-5-yl]methyl 4-decyloxybenzoate (7e)

Yield: 83.0 mg, 60%; white solid; mp 102.5 °C; Anal. Found: C, 74.15; H, 9.13; N, 2.54; calc. for C₃₄H₄₉NO₅: C, 74.01; H, 8.95; N, 2.54%; IR ν_{\max} /cm⁻¹: 2924, 2854, 1715, 1606, 1510, 1466, 1377, 1249, 1169, 1127, 1014, 882, 834, 768, 722, 699, 666, 649; ¹H NMR (300 MHz, CDCl₃) δ 0.89 (m, 6H, (CH₃)₂), 1.38 (m, 22H, (CH₂)₁₁), 1.79 (m, 4H, (CH₂CH₂O)₂), 3.22 (dd, *J* 16.5, 6.9 Hz, 1H, N=CCH₂HCH), 3.49 (dd, *J* 16.5, 10.8 Hz, 1H, N=CCH₂HCH), 3.98 (t, *J* 6.6 Hz, 4H, (CH₂O)₂), 4.44 (m, 2H, CHCH₂OCO), 5.06 (m, 1H), 6.85 (d, *J* 8.7 Hz, 2H, Ar), 6.91 (d, *J* 8.4 Hz, 2H, Ar), 7.61 (d, *J* 8.7 Hz, 2H, Ar), 7.95 (d, *J* 9.0 Hz, 2H, Ar); ¹³C NMR (75 MHz, CDCl₃) δ 14.0, 14.1, 22.5, 22.6, 25.9, 28.9, 29.0, 29.1, 29.2, 29.3, 29.5, 31.7, 31.8, 37.6, 65.2, 68.0,

68.1, 78.0, 114.0, 114.6, 121.5, 121.6, 128.2, 131.7, 155.8, 160.7, 163.1, 166.0; EI-MS: *m/z* 436, 360, 325, 291, 290, 277, 274, 260, 235 (100), 190, 156, 116 and 91.

General procedure of the series 8a-d

(i) Esterification reaction: alcohol **2a** (4.4 mmol) and *p*-bromobenzoic acid (4.4 mmol) were suspended in dry THF (30 mL) and stirred for 15 min under argon atmosphere. Then DCC (6.6 mmol) and DMAP (0.58 mmol) were added. The reaction mixture was stirred for 24 h at room temperature. The white precipitate was filtered off and washed with THF. The solvent from the filtrate was removed and the solid was recrystallized twice from ethanol to afford the corresponding esters as white crystals in 70-90% of yield. All the compounds gave satisfactory analytical data. (ii) Sonogashira's coupling: A one-neck round-bottom flask equipped with septum stoppers was charged with the ester produced in step (i) (0.8 mmol), the corresponding 1-alkoxy-4-ethynylbenzene (1.2 mmol) and Et₃N (20 mL) under argon atmosphere. The suspension was stirred for 20 min and then CuI (1.2×10^{-5} mol), PPh₃ (4.0×10^{-5} mol) and [PdCl₂(PPh₃)₂] (0.8×10^{-5} mol) were added. The mixture was heated under reflux for 48 h. The solution was cooled to room temperature and the solid was filtered through a Celite[®] pad and washed with diethyl ether (2 \times 100 mL). The filtrate was then extracted with H₂O (4 \times 20 mL) and the organic extracts were dried (Na₂SO₄) and the solvent evaporated. The solid was recrystallized in ethanol affording the respective products.

Representative data for [3-(4-heptyloxyphenyl)-4,5-dihydroisoxazol-5-yl]methyl 4-[(octyl oxyphenyl)ethynyl]benzoate (8b)

Yield: 63 mg, 40%; orange solid; mp 138.4 °C; Anal. Found: C, 76.96; H, 8.07; N, 2.14; calc. for C₄₀H₄₉NO₅: C, 77.01; H, 7.92; N, 2.25%; IR ν_{\max} /cm⁻¹: 2924, 2855, 1723, 1600, 1517, 1465, 1377, 1286, 1251, 1177, 1108, 1045, 890, 834, 765, 721, 695, 666; ¹H NMR (300 MHz, CDCl₃) δ 0.89 (m, 6H, (CH₃)₂), 1.38 (m, 18H, (CH₂)₉), 1.79 (m, 4H, (CH₂CH₂O)₂), 3.24 (dd, 1H, N=CCH₂HCH, *J* 16.5, 6.6 Hz), 3.52 (dd, 1H, N=CCH₂HCH, *J* 16.5, 10.5 Hz), 3.98 (m, 4H, (CH₂O)₂), 4.43 (dd, 1H, CHCH₂HOCO, *J* 12.0, 5.4 Hz), 4.50 (dd, 1H, CHCH₂HOCO, *J* 12.0, 4.2 Hz), 5.08 (m, 1H), 6.87 (d, 2H, Ar, *J* 9.0 Hz), 6.92 (d, 2H, Ar, *J* 8.7 Hz), 7.45 (d, 2H, Ar, *J* 9.0 Hz), 7.51 (d, 2H, Ar, *J* 8.4 Hz), 7.62 (d, 2H, Ar, *J* 9.0 Hz), 7.97 (d, 2H, Ar, *J* 8.4 Hz); ¹³C NMR (75 MHz, CDCl₃) δ 14.0, 22.5, 22.6, 25.8, 25.9, 28.9, 29.0, 29.1, 29.3, 31.6, 31.7, 37.5, 65.7, 68.0, 77.8, 87.3, 92.9, 114.3, 114.5, 114.6, 121.3, 128.1, 128.3, 128.6, 129.6, 131.2, 133.1, 155.8, 159.6, 160.7, 165.7; EI-MS: *m/z* 624

([M + H]⁺), 623 [M⁺], 430, 364, 349, 333, 306, 290, 274, 260, 234 (100), 230, 204, 190, 116 and 91.

Conclusions

In this work a molecular platform for liquid-crystalline materials based on 3-arylisoxazolyl-5-carboxylic acid and 5-(hydroxymethyl)-3-aryl-2-isoxazoline was described. In this context, a new series of liquid-crystalline **5a-c**, **6a**, **7a-g** and **8a-d** derived from isoxazolinic molecular platforms were synthesized and their mesomorphic behavior was investigated using POM and DSC techniques. The compounds belonging to series **5a-c** showed an enantiotropic nematic phase while **6** was not mesogenic. The monotropic smectic C phase of the third series was observed in **7c-g**. The first two **7a-b** did not exhibit a smectic LC phase. The last series **8a-d** displayed a monotropic nematic phase. A theoretical study was performed in order to understand the phase behavior and structural features of these compounds. The reported calculations further support the role of the insertion of a methylene unit between the isoxazoline ring and the carboxylate group disfavoring the molecular interaction in the liquid-crystalline state.

Acknowledgments

This work was supported by Conselho Nacional de Desenvolvimento Científico e Tecnológico (project MCT/CNPq No. 555785/2006-8 and MCT/CNPq Universal No. 471194/2008-5), PROCAD-CAPEs, INCT-CMN/CNPq and Coordenação de Aperfeiçoamento de Pessoal de Nível Superior (CAPES) for fellowship.

Supplementary Information

Copies of ¹H NMR, ¹³C NMR spectrum and ESI-MS are available free of charge at <http://jbc.sqb.org.br>, as PDF file.

References

- Carmella, P.; Grünanger, P.; *1,3-Dipolar Cycloaddition Chemistry*; Padwa, A., ed.; Wiley: New York, 1984; vol. 1, pp. 291-392; Torsell, K. B. G.; *Nitrile Oxides, Nitrones and Nitronates*; VCH: Weinheim, 1988.
- Kozikowski, A. P.; *Acc. Chem. Res.* **1984**, *17*, 410; Jager, V.; Muller, I.; *Tetrahedron* **1985**, *41*, 3519.
- Curran, D. P.; Zhang, J.; *J. Chem. Soc. Perkin Trans. I* **1991**, 2613.
- Kenar, J. A.; *J. Am. Oil Chem. Soc.* **2002**, *79*, 351.
- Kovganko, V. N.; Kovganko, N. N.; *Russ. J. Org. Chem.* **2006**, *42*, 696; Ritter, O. M. S.; Giacomelli, F. C.; Passo, J. A.; Silveira, N. P.; Merlo, A. A.; *Polym. Bull.* **2006**, *56*, 549; Kauhanka, U. M.; Kauhanka, M. M.; *Liq. Cryst.* **2006**, *33*, 121; Bezborodov, V.; Kauhanka, N.; Lapanik, V.; *Mol. Cryst. Liq. Cryst.* **2004**, *411*, 1145; Merlo, A. A.; Gallardo, H.; Taylor, T. R.; *Quim. Nova* **2001**, *24*, 354.
- Tavares, A.; Schneider, P. H.; Merlo, A. A.; *Eur. J. Org. Chem.* **2009**, 889; Passo, J. A.; Vilela, G. D.; Schneider, P. H.; Ritter, O. M. S.; Merlo, A. A.; *Liq. Cryst.* **2008**, *35*, 833; Gallardo, H.; Conte, G.; Bryk, F.; Lourenço, M. C. S.; Costa, M. S.; Ferreira, V. F.; *J. Braz. Chem. Soc.* **2007**, *18*, 1285.
- Gimeno, N.; Ros, M. B.; De la Fuente, M. R.; Serrano, J. L.; *Chem. Mater.* **2008**, *20*, 1262; Naoum, M. M.; Saad, G. R.; Nessim, R. I.; Abdel Aziz, T. A.; Seliger, H.; *Liq. Cryst.* **1997**, *23*, 789.
- Vasconcelos, U. B.; Dalmolin, E.; Merlo, A. A.; *Org. Lett.* **2005**, *7*, 1027; Vasconcelos, U. B.; Merlo, A. A.; *Synthesis* **2006**, *7*, 1141; Vasconcelos, U. B.; Vilela, G. D.; Schrader, A.; Borges, A. C. A.; Merlo, A. A.; *Tetrahedron* **2008**, *64*, 4619; Sonogashira, K.; Tohda, Y.; Hagihara, N.; *Tetrahedron Lett.* **1975**, *16*, 4467; Chinchilla, R.; Nájera, C.; *Chem. Rev.* **2007**, *107*, 874; Cristiano, R.; Santos, D. M. P. O.; Conte, G.; Gallardo, H.; *Liq. Cryst.* **2006**, *33*, 997; Melissaris, A. P.; Litt, M. H.; *Macromolecules* **1994**, *27*, 883.
- Gray, G. W.; Goodby, J. W. G.; *Smectic Liquid Crystals. Textures and Structures*; Leonard Hill: London, 1984.
- Frisch, M. J.; Trucks, G. W.; Schlegel, H. B.; Scuseria, G. E.; Robb, M. A.; Cheeseman, J. R.; Zakrzewski, V. G.; Montgomery J. A.; Stratmann, Jr., R. E.; Burant, J. C.; Dapprich, S.; Millam, J. M.; Daniels, A. D.; Kudin, K. N.; Strain, M. C.; Farkas, O.; Tomasi, J.; Barone, V.; Cossi, M.; Cammi, R.; Mennucci, B.; Pomelli, C.; Adamo, C.; Clifford, S.; Ochterski, J.; Petersson, G. A.; Ayala, P. Y.; Cui, Q.; Morokuma, K.; Malick, D. K.; Rabuck, A. D.; Raghavachari, K.; Foresman, J. B.; Cioslowski, J.; Ortiz, J. V.; Stefanov, B. B.; Liu, G.; Liashenko, A.; Piskorz, P.; Komaromi, I.; Gomperts, R.; Martin, R. L.; Fox, D. J.; Keith, T.; Al-Laham, M. A.; Peng, C. Y.; Nanayakkara, A.; Gonzalez, C.; Challacombe, M.; Gill, P. M. W.; Johnson, B.; Chen, W.; Wong, M. W.; Andres, J. L.; Gonzalez, C.; Head-Gordon, M.; Replogle, E. S.; Pople, J. A.; *Gaussian 98, Revision A.5*. Gaussian, Inc.: Pittsburgh, PA., 1998; Becke, A. D.; *J. Chem. Phys.* **1993**, *98*, 5648; Lee, C.; Yang, W.; Parr, R. G.; *Phys. Rev. B* **1988**, *37*, 785.
- Dingemans, T. J.; Samulski, E. T.; *Liq. Cryst.* **2000**, *27*, 131; Cai, R.; Samulsky, E. T.; *Liq. Cryst.* **1991**, *9*, 617.
- Vieira, A.; Bryk, F.; Conte, G.; Bortoluzzi, A.; Gallardo, H.; *Tetrahedron Lett.* **2009**, *50*, 905; Gallardo, H.; Cristiano, R.; Ely, F.; Vieira, A.; *Liq. Cryst.* **2006**, *33*, 381.
- King, A. O.; Negishi, E.; *J. Org. Chem.* **1978**, *43*, 358.

Received: March 31, 2009

Web Release Date: September 25, 2009

3-Arylisoxazolyl-5-Carboxylic Acid and 5-(Hydroxymethyl)-3-Aryl-2-Isoxazoline as Molecular Platforms for Liquid-crystalline Materials

Aline Tavares,^a Paolo R. Livotto,^a Paulo F. B. Gonçalves^b and Aloir A. Merlo^{*,a}

^aInstituto de Química, Universidade Federal do Rio Grande do Sul, 91501-970 Porto Alegre-RS, Brazil

^bCentro Universitário La Salle, 92010-000 Canoas-RS, Brazil

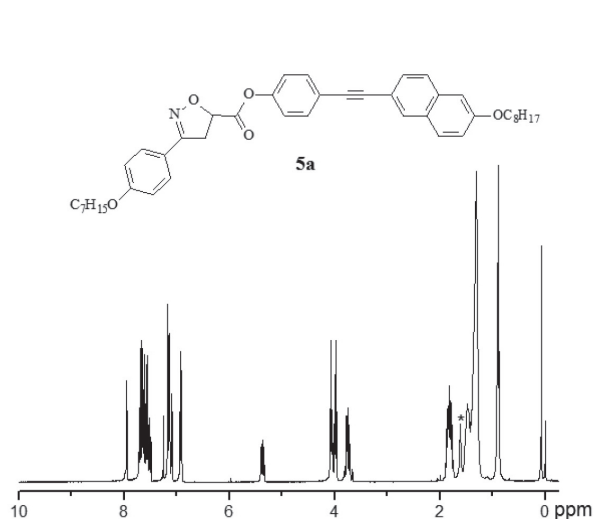


Figure S1. ¹H NMR spectrum of compound **5a** (CDCl₃, 300 MHz).
*Solvent impurity.

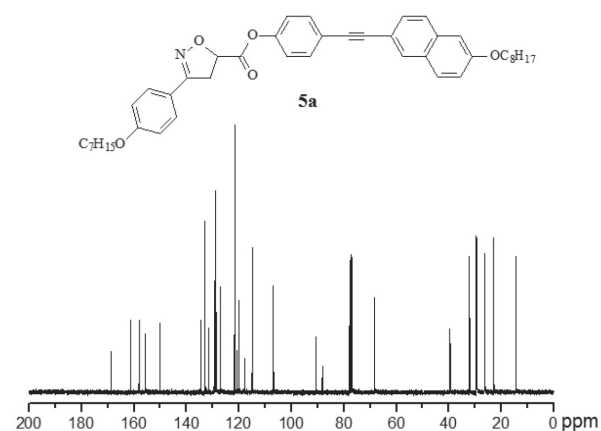


Figure S2. ¹³C NMR spectrum of compound **5a** (CDCl₃, 75 MHz).

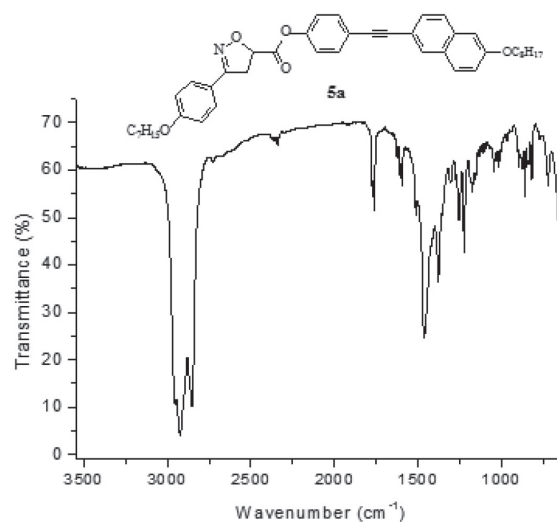


Figure S3. FT-IR spectrum of compound **5a** (nujol).

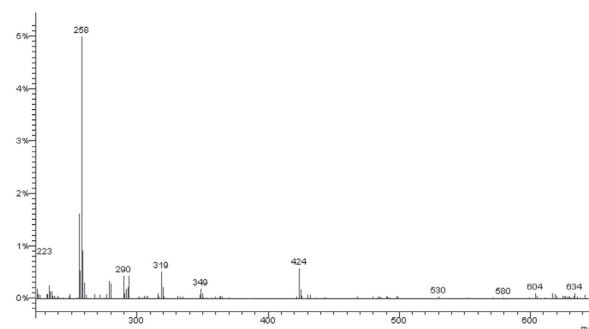


Figure S4. Mass spectra (EI-MS) of compound **5a**.

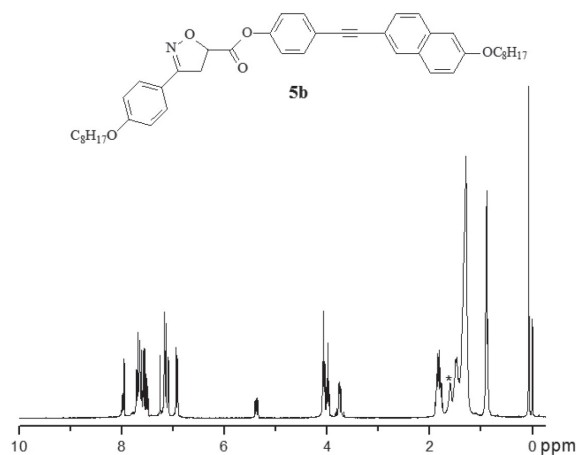


Figure S5. ^1H NMR spectrum of compound **5b** (CDCl_3 , 300 MHz).
*Solvent impurity.

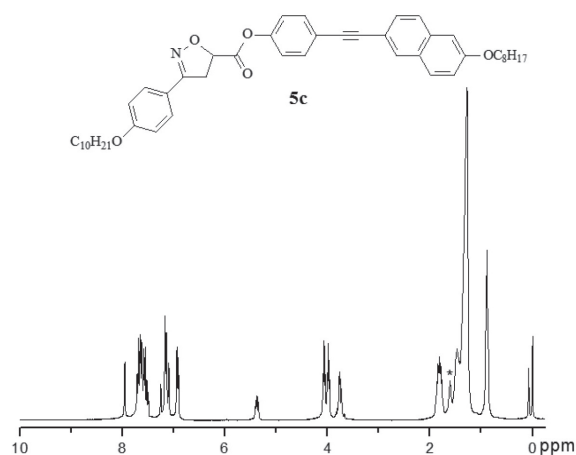


Figure S8. ^1H NMR spectrum of compound **5c** (CDCl_3 , 300 MHz).
*Solvent impurity.

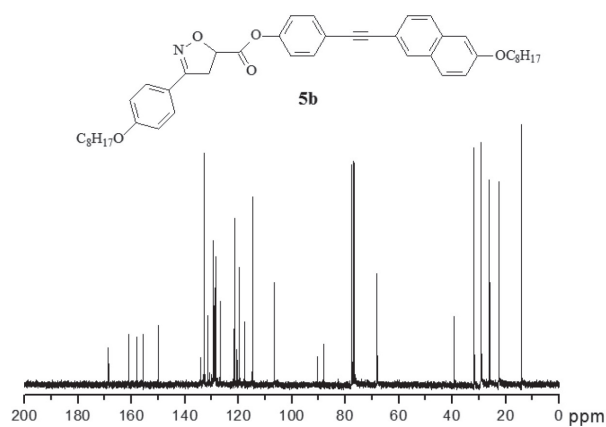


Figure S6. ^{13}C NMR spectrum of compound **5b** (CDCl_3 , 75 MHz).

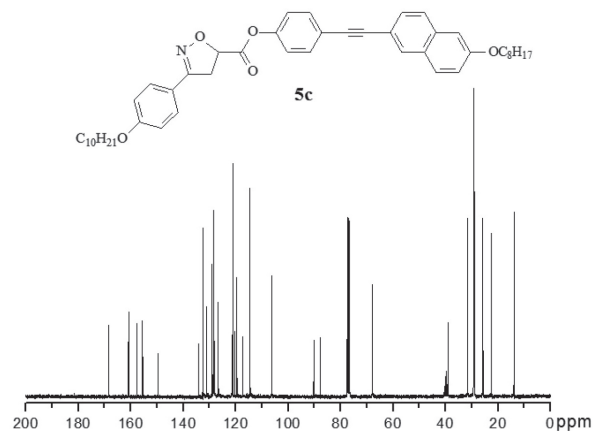


Figure S9. ^{13}C NMR spectrum of compound **5c** ($\text{CDCl}_3/\text{DMSO}-d_6$, 75 MHz).

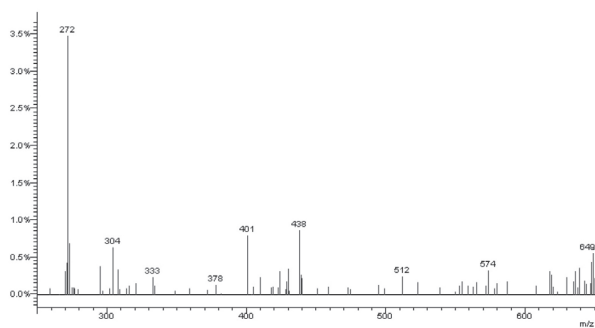


Figure S7. Mass spectra (EI-MS) of compound **5b**.

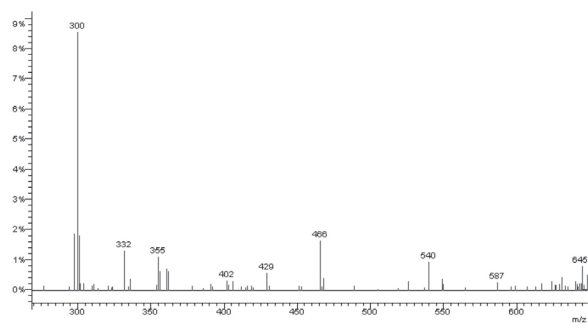


Figure S10. Mass spectra (EI-MS) of compound **5c**.

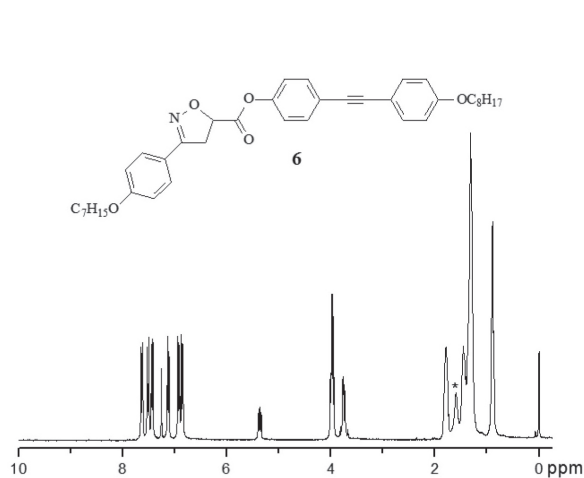


Figure S11. ^1H NMR spectrum of compound **6** (CDCl_3 , 300 MHz).
*Solvent impurity.

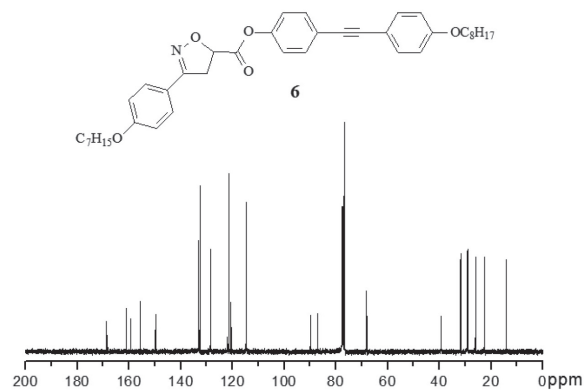


Figure S12. ^{13}C NMR spectrum of compound **6** (CDCl_3 , 75 MHz).

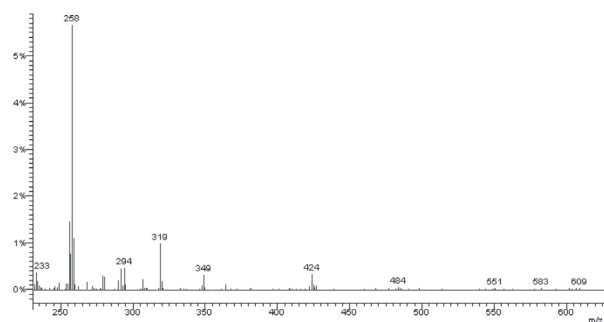


Figure S13. Mass spectra (EI-MS) of compound **6**.

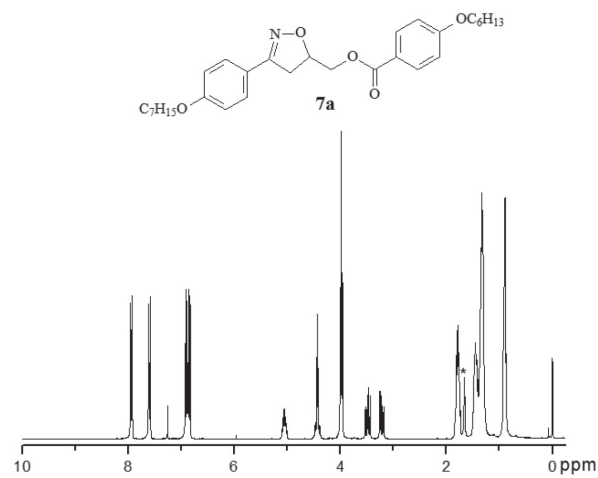


Figure S14. ^1H NMR spectrum of compound **7a** (CDCl_3 , 300 MHz).
*Solvent impurity

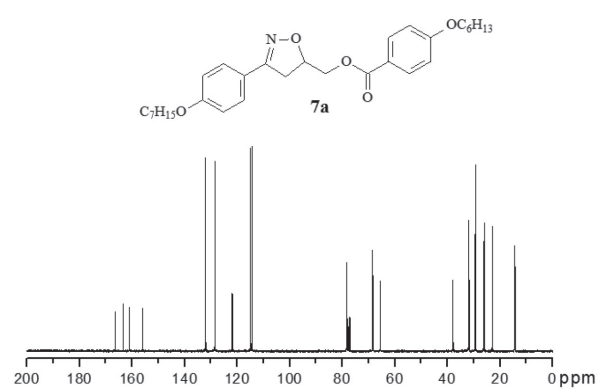


Figure S15. ^{13}C NMR spectrum of compound **7a** (CDCl_3 , 75 MHz).

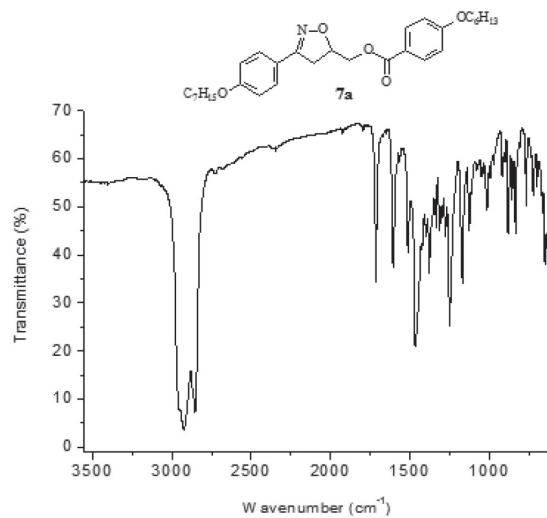


Figure S16. FT-IR spectrum of compound **7a** (nujol).

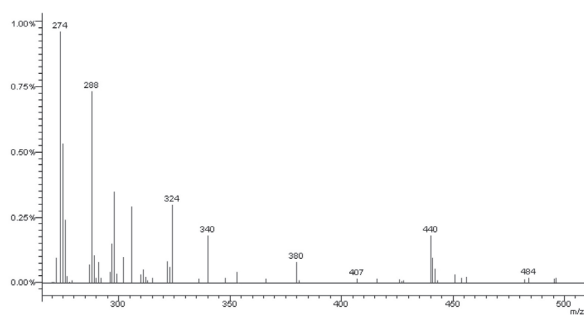


Figure S17. Mass spectra (EI-MS) of compound **7a**.

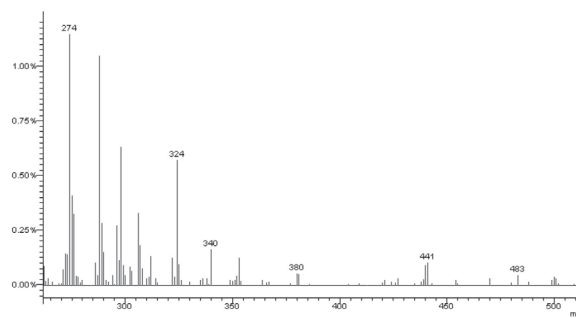


Figure S20. Mass spectra (EI-MS) of compound **7b**.

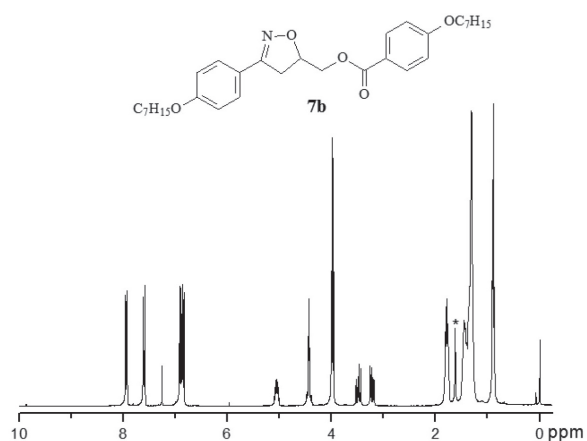


Figure S18. ^1H NMR spectrum of compound **7b** (CDCl_3 , 300 MHz).
*Solvent impurity.

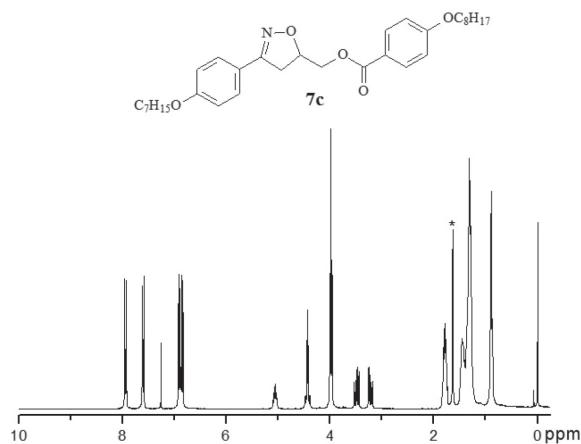


Figure S21. ^1H NMR spectrum of compound **7c** (CDCl_3 , 300 MHz).
*Solvent impurity.

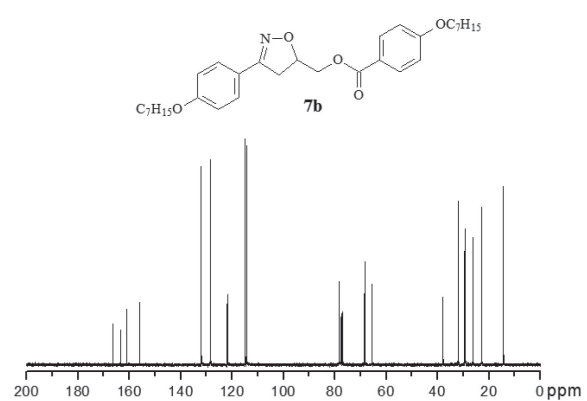


Figure S19. ^{13}C NMR spectrum of compound **7b** (CDCl_3 , 75 MHz).

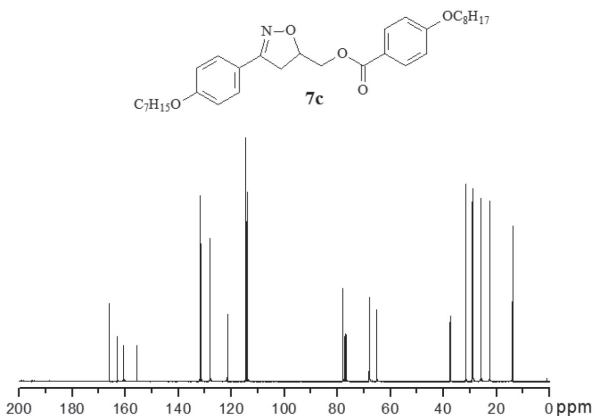


Figure S22. ^{13}C NMR spectrum of compound **7c** (CDCl_3 , 75 MHz).

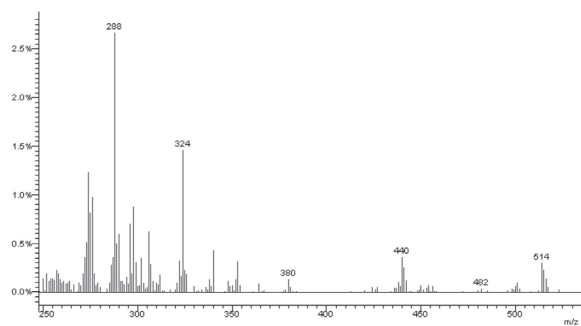


Figure S23. Mass spectra (EI-MS) of compound **7c**.

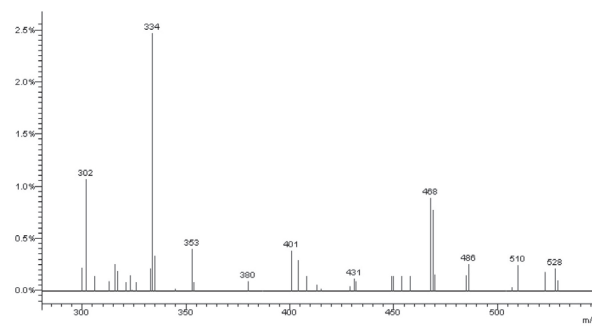


Figure S26. Mass spectra (EI-MS) of compound **7d**.

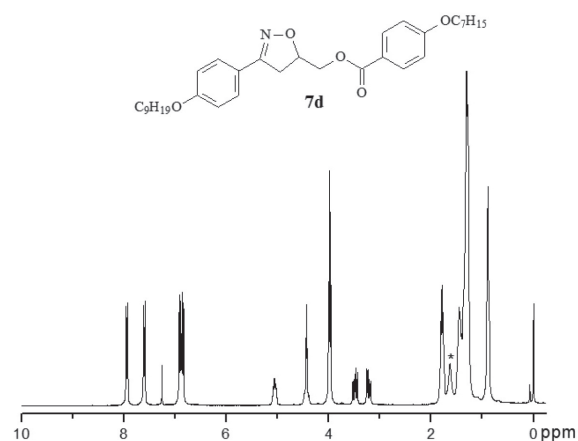


Figure S24. ^1H NMR spectrum of compound **7d** (CDCl_3 , 300 MHz).
*Solvent impurity.

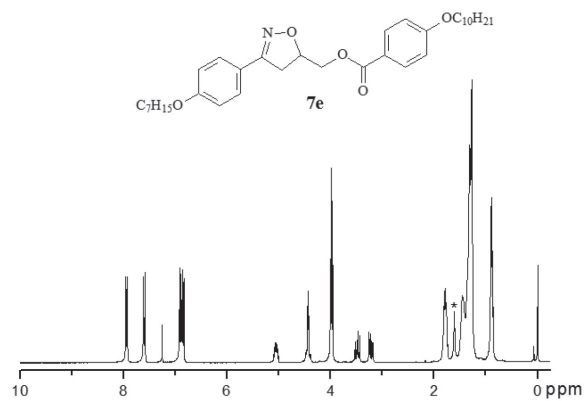


Figure S27. ^1H NMR spectrum of compound **7e** (CDCl_3 , 300 MHz).
*Solvent impurity.

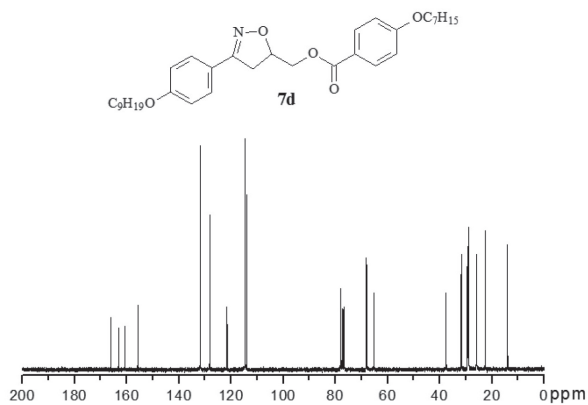


Figure S25. ^{13}C NMR spectrum of compound **7d** (CDCl_3 , 75 MHz).

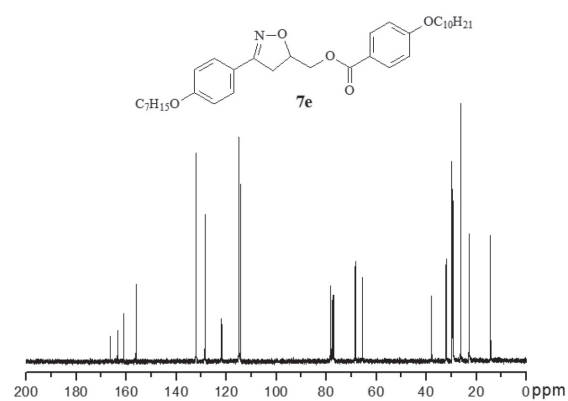


Figure S28. ^{13}C NMR spectrum of compound **7e** (CDCl_3 , 75 MHz).

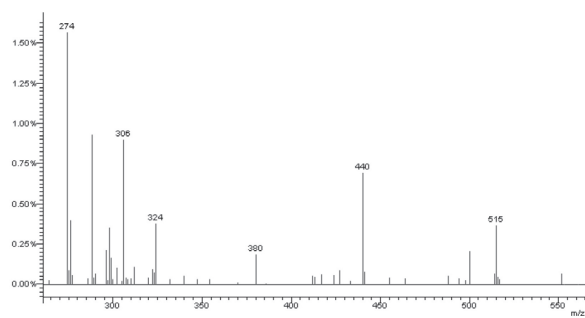


Figure S29. Mass spectra (EI-MS) of compound 7e.

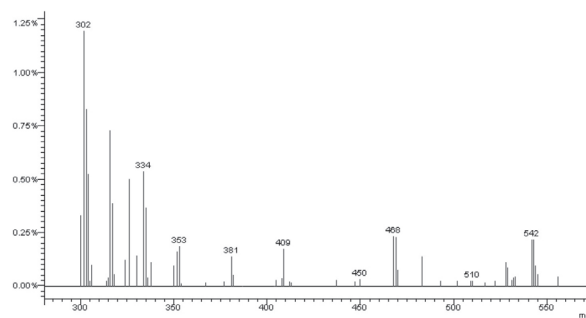
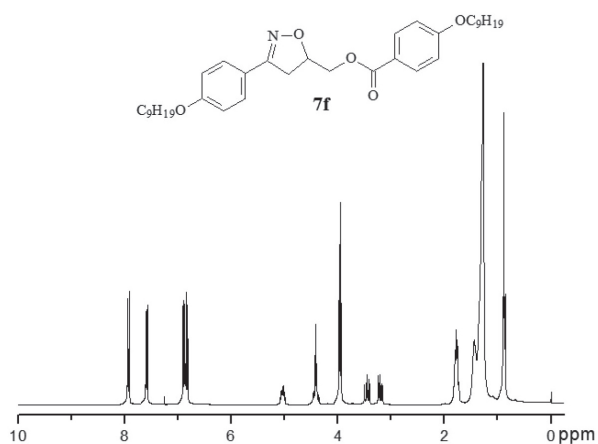
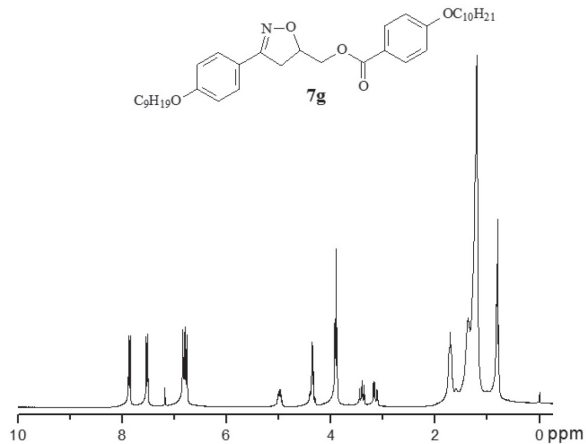
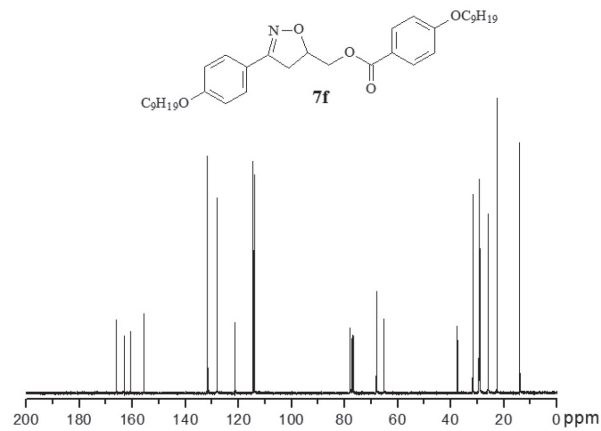
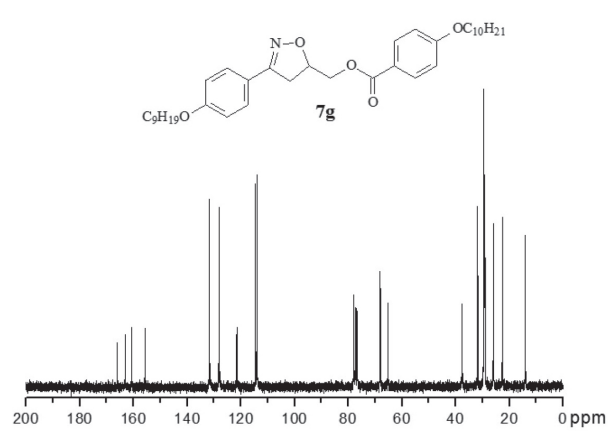


Figure S32. Mass spectra (EI-MS) of compound 7f.

Figure S30. ^1H NMR spectrum of compound 7f (CDCl_3 , 300 MHz).Figure S33. ^1H NMR spectrum of compound 7g (CDCl_3 , 300 MHz).Figure S31. ^{13}C NMR spectrum of compound 7f (CDCl_3 , 75 MHz).Figure S34. ^{13}C NMR spectrum of compound 7g (CDCl_3 , 75 MHz).

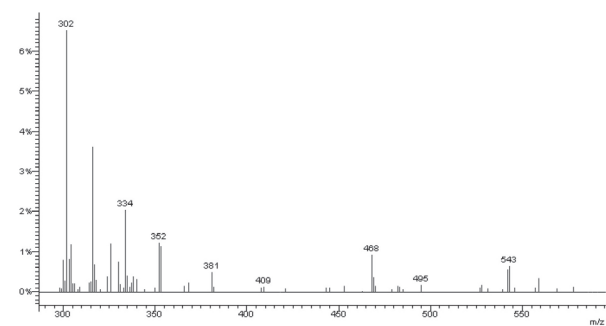


Figure S35. Mass spectra (EI-MS) of compound **7g**.

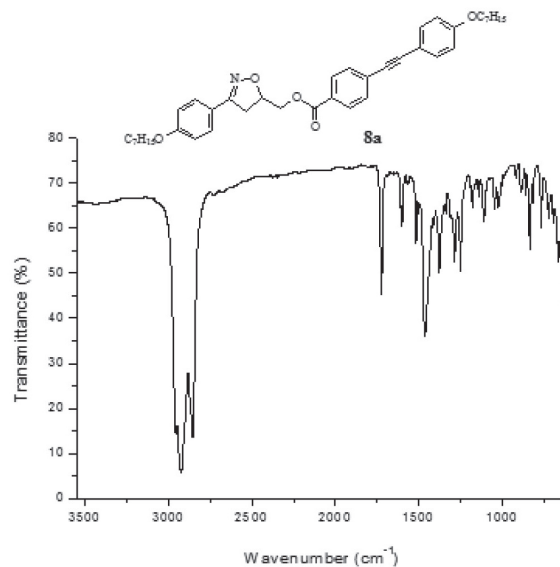


Figure S38. FT-IR spectrum of compound **8a** (nujol).

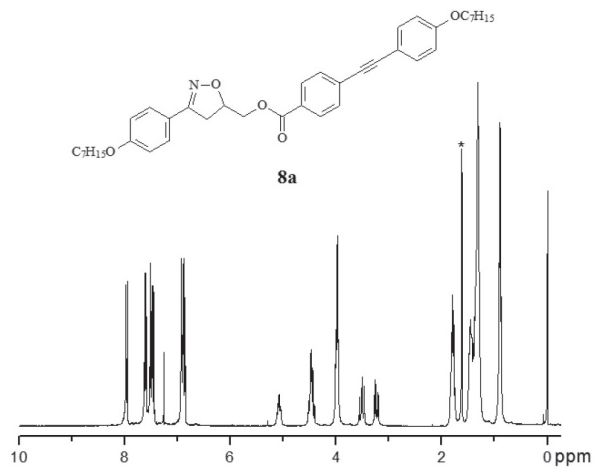


Figure S36. ¹H NMR spectrum of compound **8a** (CDCl₃, 300 MHz).
*Solvent impurity.

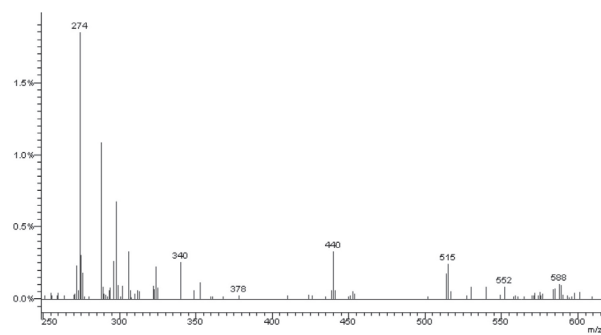


Figure S39. Mass spectra (EI-MS) of compound **8a**.

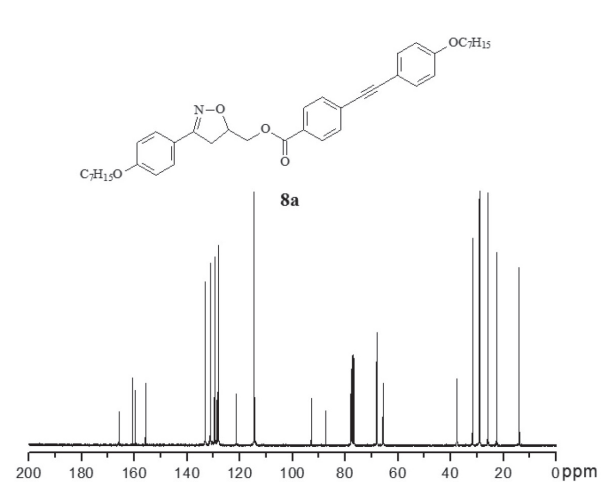


Figure S37. ¹³C NMR spectrum of compound **8a** (CDCl₃, 75 MHz).

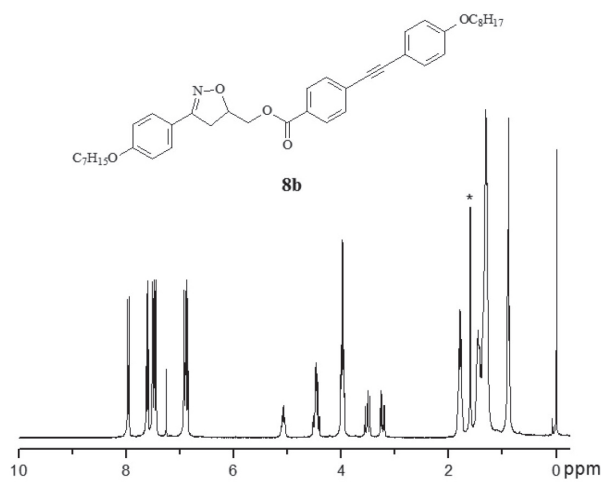


Figure S40. ¹H NMR spectrum of compound **8b** (CDCl₃, 300 MHz).
*Solvent impurity.

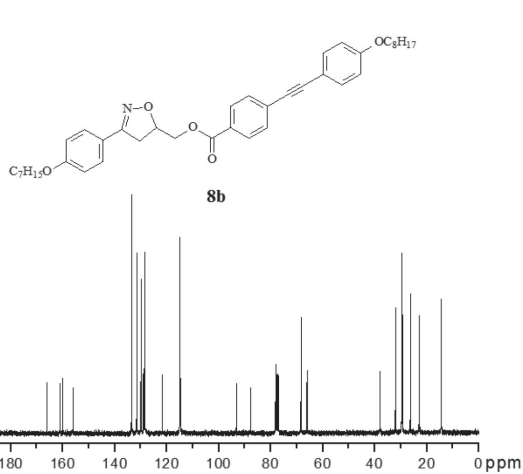


Figure S41. ^{13}C NMR spectrum of compound **8b** (CDCl_3 , 75 MHz).

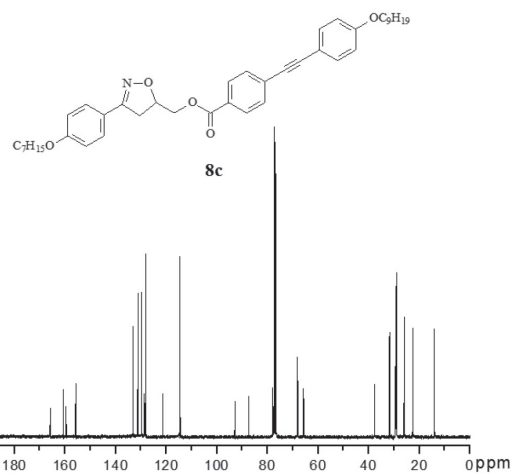


Figure S44. ^{13}C NMR spectrum of compound **8c** (CDCl_3 , 75 MHz).

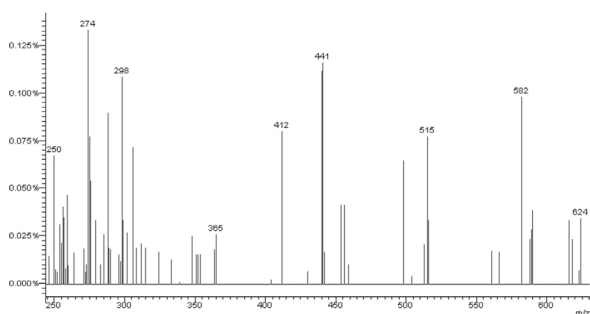


Figure S42. Mass spectra (EI-MS) of compound **8b**.

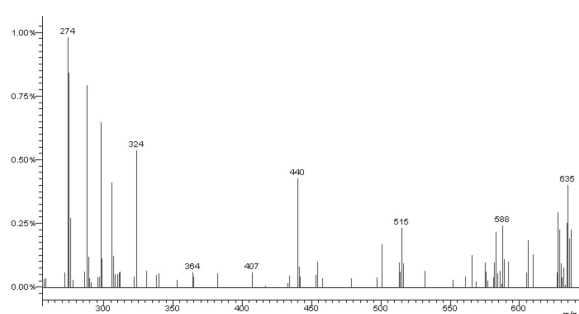


Figure S45. Mass spectra (EI-MS) of compound **8c**.

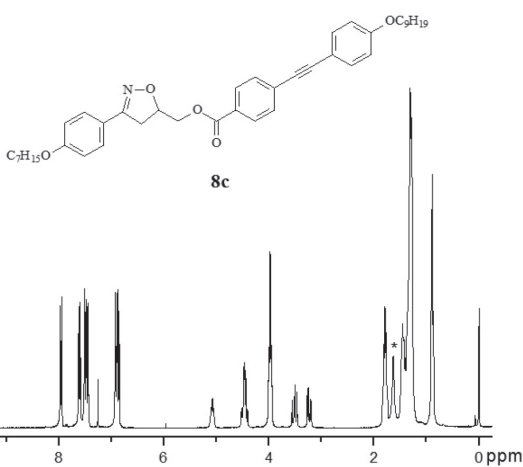


Figure S43. ^1H NMR spectrum of compound **8c** (CDCl_3 , 300 MHz).
*Solvent impurity.

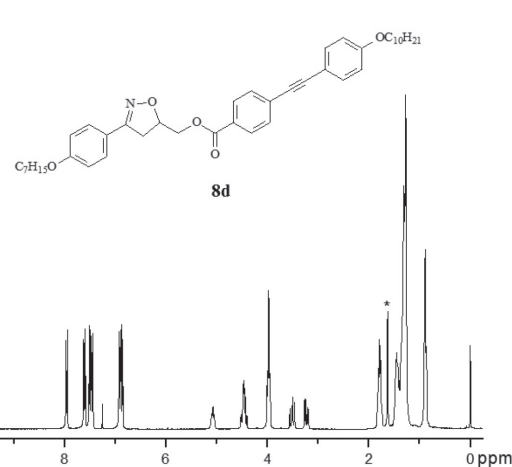


Figure S46. ^1H NMR spectrum of compound **8d** (CDCl_3 , 300 MHz).
*Solvent impurity.

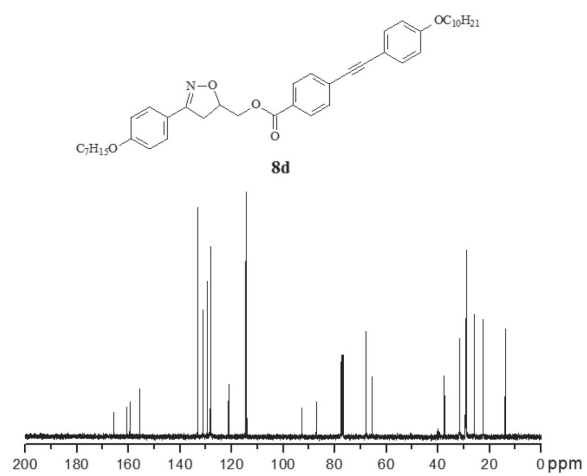


Figure S47. ¹³C NMR spectrum of compound **8d** (CDCl₃/DMSO-d₆, 75 MHz).

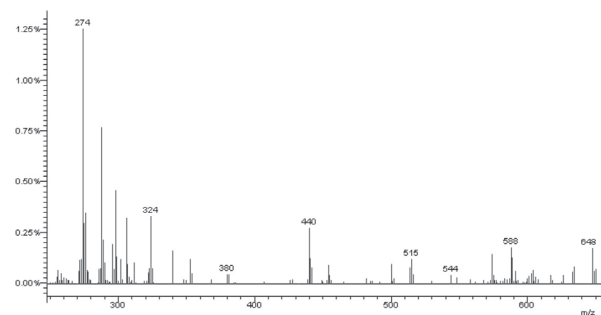


Figure S48. Mass spectra (EI-MS) of compound **8d**.